# Chiral Template-Directed Regio-, Diastereo-, and Enantioselective Photodimerization of an Anthracene Derivative Assisted by Complementary Amidinium–Carboxylate Salt Bridge Formation

Junki Tanabe, Daisuke Taura,[†] Naoki Ousaka,[†] and Eiji Yashima*,[†]

Department of Molecular Design and Engineering, Graduate School of Engineering, Nagoya University, Chikusa-ku, Nagoya 464-8603, Japan

**ABSTRACT:** A series of optically-active amidine dimers composed of *m*-terphenyl backbones joined by a variety of linkers, such as achiral and chiral *p*-phenylene and chiral amide linkers, were synthesized and used as templates for the regio- (head-to-tail (HT) or head-to-head (HH)), diastereo- (*anti* or *syn*), and enantioselective [4 + 4] photocyclodimerization of an achiral *m*-terphenyl-based carboxylic acid monomer bearing a prochiral 2-substituted anthracene at one end (**1**) through complementary amidinium–carboxylate salt bridges. The amidine dimers linked by *p*-phenylene linkages almost exclusively afforded the chiral *syn*-HT and *anti*-HH dimers at 25 °C, while those joined by amide linkers produced all four dimers. The *p*-phenylene-linked templates tended to enhance the *syn*-HT-photodimer formation at high temperatures with no significant changes in the product enantiomeric excess (ee), while the *anti*-HH-photodimer formation remarkably increased with the decreasing temperature accompanied by a significant enhancement of the product ee up to –86% at –50 °C. Temperature-dependent inversion of the chirality of the *anti*-HH dimer was observed when the chiral phenylene-linked amidine dimer was used and the product ee was changed from 22% at 50 °C to –86 % at –50 °C. A similar enhancement of the enantioselectivity of the *anti*-HH dimer was also observed for the chiral amide-linked template, producing the *anti*-HH dimer with up to –88 % ee at –50 °C. The observed difference in the regio-, diastereo-, and enantioselectivities due to the difference in the linker structures of the amidine dimers during the template-directed photodimerization of **1** was discussed based on a reversible conformational change in the amidine dimers complexed with **1**.

## INTRODUCTION

Photochemical reactions have become one of the emerging research areas in modern synthetic chemistry during the past decade because they can promote the formation of products that are difficult to produce by thermal reactions, and the use of additional reagents, such as metal species as a catalyst, is not necessary.[1] Therefore, photochemical reactions are also attractive in the context of green chemistry. However, it still remains difficult to achieve efficient photochemical transformations with a controlled selectivity and specificity in homogeneous solutions due to the difficulty in controlling the photochemical reactions in the excited state. In order to overcome this problem, the template-directed photoreactions using noncovalent supramolecular interactions, such as hydrogen bonding and electrostatic interactions as well as metal coordination, have been developed through which the efficiency of the photoreactions has been significantly improved accompanied by an improvement in the regio- and stereoselectivities of the products.[2]

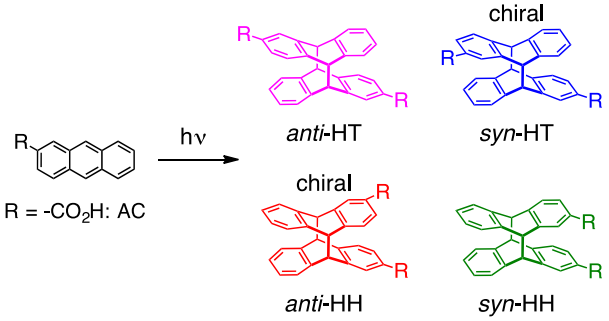


**Figure 1.** Photodimerization of 2-substituted anthracene derivatives.

The [4 + 4] photodimerization of anthracene derivatives is one of the most well-studied photochemical reactions.[3] In general, the [4 + 4] photodimerizations of substituted anthracene derivatives promote the formation of specific regio- and/or stereoisomers depending on the positions of the substituents. Therefore, the regio- and/or stereoselective template-directed photodimerizations of anthracene derivatives have been extensively investigated based on the supramolecular approach.[4–12]

**Chart 1. Structures of 2-Substituted Anthracene-Bound Monomers and Monomeric and Dimeric Amidine Templates**

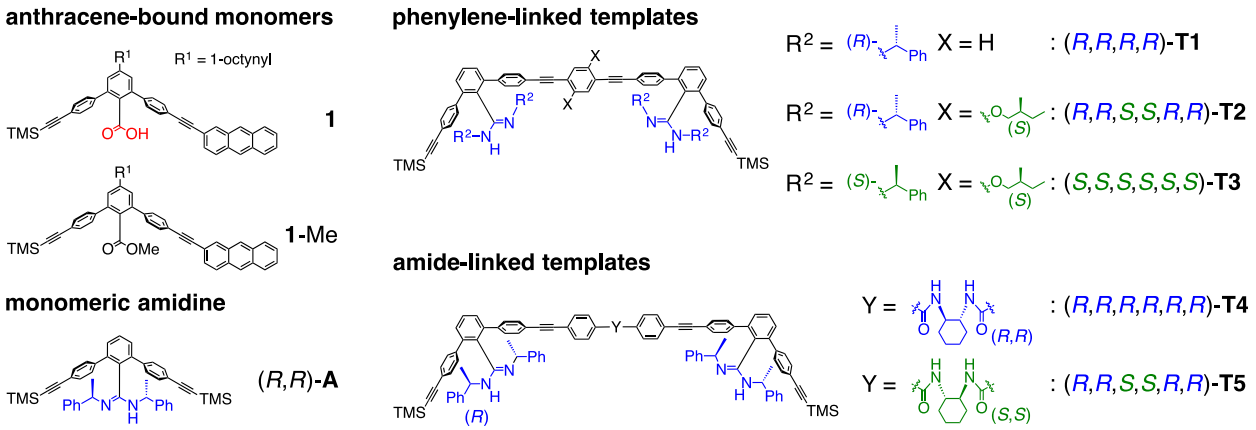


Since the first example of the enantioselective [4 + 4] photodimerizations of 1- and 2-anthracene derivatives using γ-cyclodextrin (γ-CyD) as a chiral host or template was reported by Tamaki and co-workers,[4] noticeable progress has been made in developing more efficient chiral templates or supramolecular chiral systems that can control the photodimerization of prochiral anthracenes in a highly stereospecific manner.[5–12]

Inoue and co-workers have extensively investigated the enantiodifferentiating [4 + 4] photodimerization of 2-anthracenecarboxylic acid (AC) (Figure 1) mediated by various chiral supramolecular hosts or templates, such as the modified γ-CyDs,[8] chiral hydrogen-bonding templates,[9] and proteins,[10] which produced the chiral *syn*-head-to-tail (HT) and *anti*-head-to-head (HH) dimers with moderate to high enantiomeric excess (ee) values. Interestingly, inversion of the enantioselectivity of the *anti*-HH dimer took place simply by changing the irradiation temperature or solvent when diamino-[8c] or diguanidino-γ-CyD[8j] was used as the template. Ishida, Saigo, and co-workers demonstrated that liquid crystal (LC) phases formed from the amphiphilic salts composed of amphiphilic chiral amino alcohols can be used as an asymmetric induction field, in which the photodimerization of AC took place in a highly HH-selective manner with an excellent enantioselectivity with up to 86% ee,[11] which completely inverted to –94% ee once the LC salt was isothermally annealed.[11c] As anticipated, almost perfect stereocontrol of the photodimerization of AC was achieved when two AC units were covalently attached to chiral scaffolds,[12] such as the 4,6-*O*-benzylidene-α-D-glucopyranoside, resulting in the formation of the *anti*-HH dimer in 96% yield with > 99% ee in MeOH at –70 °C.[12c]

A number of synthetic templates capable of hydrogen bonding has also been designed and synthesized for the stereoselective photodimerizations of substituted anthracenes.[6] Inoue and co-workers reported the exclusive HH-selective and highly enantioselective photodimerization of AC in the presence of prolinol,[9e] quantitatively producing the chiral *anti*-HH and achiral *syn*-HH dimers with up to 72% ee (*anti*-HH dimer).

Based on this information, we recognized that there has been a number of studies dealing with the chiral template-directed regio-, diastereo-, and enantioselectivity control during the [4 + 4] photodimerization of 2-substituted anthracenes using a variety of chiral hosts and/or templates[4,5,8-10] or in chiral reaction fields,[6,7,11] but successful examples still remain limited to modified CyDs used as a template,[8f,i,j] proteins[10b,c] as chiral biopolymer-based hosts or in chiral LC phases[11] used as an asymmetric induction field, and we are still not aware of any hydrogen bond-based template systems that achieve satisfactory regio-, diastereo-, and enantioselectivities during the photodimerization of 2-substituted anthracenes.[9] We envisaged that doubly hydrogen bonded, complementary amidinium-carboxylate salt bridges[13] would be utilized as a versatile scaffold to provide a unique and rare example of a successful template-directed photodimerization of 2-substituted anthracene derivatives, such as **1** in highly regio-, diastereo-, and enantioselective fashions, thanks to the chirality introduced on the amidine residues along with a high stability and well-defined directionality of the salt bridges.

To this end, we report the template-directed photodimerization of an *m*-terphenyl-based achiral carboxylic acid monomer (**1**) bearing a prochiral 2-substituted anthracene unit at one end

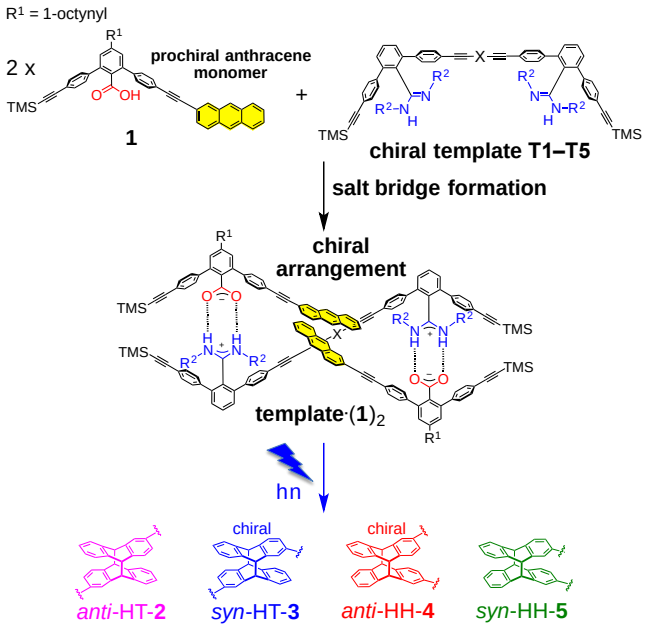


**Figure 2.** Schematic illustration for the template-directed regio-, diastereo-, and enantioselective photodimerization of 2-substituted anthracene-bound carboxylic acid monomer (**1**) using chiral amidine dimers (**T1**–**T5**) as the template.

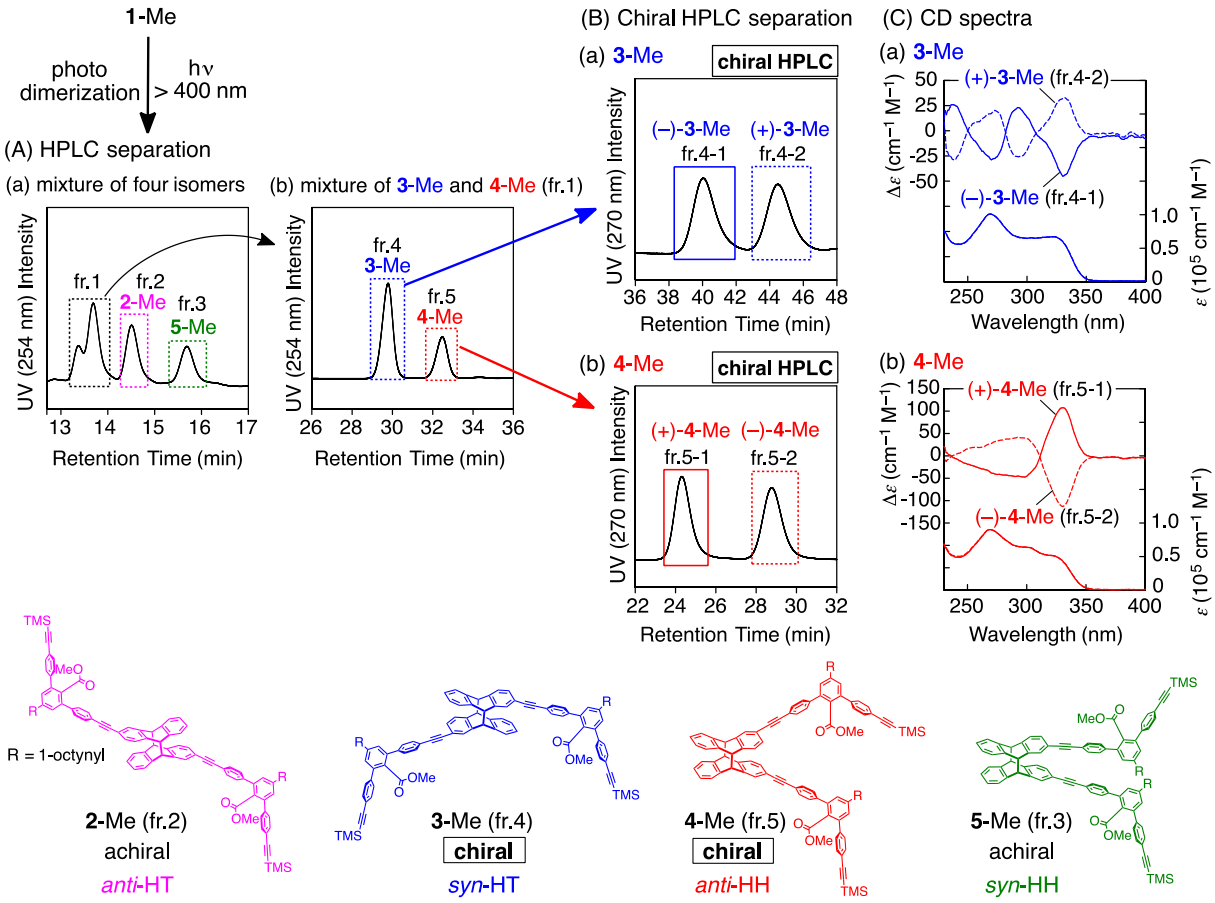


**Figure 3.** (A) HPLC chromatograms of photodimers obtained after irradiation of light (> 400 nm) of **1**-Me (8.0 mM) (a) and a mixture of **3**-Me and **4**-Me (fr.1) (b). (B) HPLC chromatograms for the resolution of the isolated **3**-Me (a) and **4**-Me (b) (for detail HPLC conditions, see SI). (C) CD and absorption spectra of (+)-**3**-Me (0.020 mM) (a, dotted line), (–)-**3**-Me (0.018 mM) (a, solid line), (+)-**4**-Me (0.018 mM) (b, solid line), and (–)-**4**-Me (0.021 mM) (b, dotted line) in $CDCl_3$ at 25 °C. + and – denote the signs of the Cotton effect at 340 nm.

in the presence of a series of optically-active amidine dimer templates (**T1**–**T5**) (Chart 1) and the effects of the linker structures and chiralities of the linkages and amidine units of the templates on the reactivity of **1**, and the regio- (HT or HH), diastereo- (*anti* or *syn*), and enantioselectivities during the photodimerization reaction were systematically investigated (Figure 2).[14] We anticipated that the photodimerization of **1** would proceed in highly regio-, diastereo-, and enantioselective fashions along the optically-active amidine dimer templates through complementary amidinium–carboxylate salt bridges, producing a specific photodimer with optical activity among six possible stereoisomers (*anti*-HT-, (+)- and (–)-*syn*-HT-, (+)- and (–)-*anti*-HH-, and *syn*-HH-dimers) (Figure 2).

## RESULTS AND DISCUSSION

**Synthesis.** A novel *m*-terphenyl-based, achiral carboxylic acid monomer (**1**) bearing a 2-substituted anthracene unit and its methyl ester (**1**-Me) used as a model monomer (Chart 1) were synthesized according to Schemes S1 and S2, respectively (see the Supporting Information [SI]). A series of optically-active amidine dimers (**T1**–**T5**) composed of (*R*)- or (*S*)-1-phenylethyl amidine with an *m*-terphenyl skeleton joined by an achiral *p*-phenylene (**T1**)[13d] and optically-active linkages, such as 2,5-di-(*S*)-2-methylbutoxyphenylene (**T2** and **T3**) and (*R*,*R*)- and (*S*,*S*)-*trans*-1,2-cyclohexanediamine through amide bonds (**T4** and **T5**, respectively),[13g,j] were also prepared in a stepwise manner mainly based on reported methods (see Schemes S3 and S4).

**Photodimerization of Model Monomer (1-Me), Isolation of Photodimers, Optical Resolution, and Structure Determination.** The photodimerization of **1**-Me (0.50 mM) was first investigated in degassed $CDCl_3$ at 25 °C upon irradiation of light over 400 nm, affording all four configurational [4 + 4] cyclophotodimers with respect to HT or HH with *anti* or *syn* isomerism, namely, the *anti*-HT-**2**-Me and *syn*-HT-**3**-Me dimers and *anti*-HH-**4**-Me and *syn*-HH-**5**-Me dimers, of which *syn*-HT-**3**-Me and *anti*-HH-**4**-Me are chiral. The time-dependent $^1$H NMR spectral changes of **1**-Me (Figure S1A) showed that the peak intensities of the anthracene protons, such as $H_a$-$H_c$ in **1**-Me, gradually decreased with time, while new signals appeared in the aromatic regions (6.8–7.2 and around 4.57 ppm), which can be assigned to the protons of the cyclodimerized-anthracene and bridge-head ($H_d$ and $H_e$) protons, respectively, suggesting the [4 + 4] photodimer formation that exclusively took place during the photodimerization of **1**-Me.[15]

The formation of cyclophotodimers was also supported by a molecular ionic peak at m/z = 1408.53 ($[C_{98}H_{88}O_4Si_2 + Na]^+$) in its positive-mode electron-spray ionization (ESI) mass spectrum (Figure S1D). Due to the $^1$H NMR spectral changes of **1**-Me, the reaction rate constant ($k$) was estimated to be $0.46 \times 10^{-3}$ $s^{-1}$ based on a first-order kinetic model (Figure S1B,C).[13k]

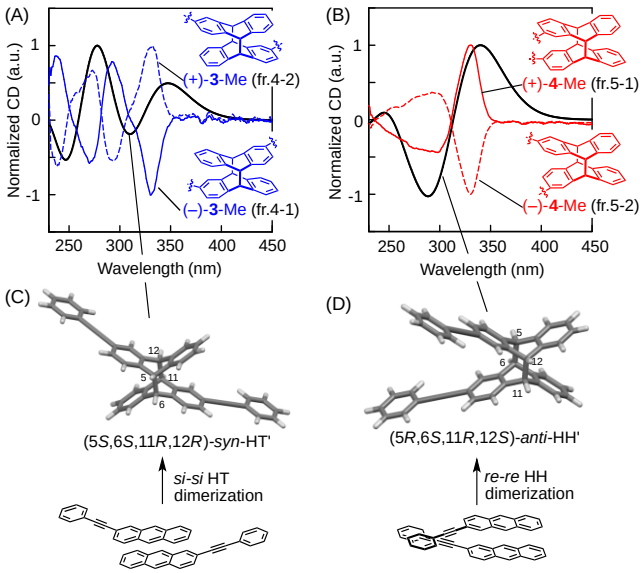


**Figure 4.** Calculated CD spectra (black lines) of chiral model photodimers of 2-phenylethynylanthracene with (5*S*,6*S*,11*R*,12*R*)-*syn*-HT' (A) and (5*R*,6*S*,11*R*,12*S*)-*anti*-HH' (B) configurations. The observed CD spectra of *syn*-HT-(+)- (blue dotted line) and (–)-**3**-Me (blue solid line) (A) and those of *anti*-HH-(+)- (red solid line) and (–)-**4**-Me (red dotted line) (B) are also shown. The CD spectra (black lines) were calculated by TD-DFT calculations at the B3LYP level and the 6-31G* basis set in Gaussian 09 software (Gaussian, Inc., Pittsburgh, PA). The resultant energy-minimized structures are depicted in (C) ((5*S*,6*S*,11*R*,12*R*)-*syn*-HT') and (D) ((5*R*,6*S*,11*R*,12*S*)-*anti*-HH'). The enantioface (*re* or *si*) is defined at the 2-position of anthracene, to which the ethynylphenyl group is attached.[9b] The calculated CD spectra of (5*S*,6*S*,11*R*,12*R*)-*syn*-HT' (*si*-*si*-stacked dimer, A) and (5*R*,6*S*,11*R*,12*S*)-*anti*-HH' (*re*-*re*-stacked dimer, B) were in good agreement with the observed CD spectra of the second-eluted (+)-enantiomer of fr.4 (Figure 3Ba) and the first-eluted (+)-enantiomer of fr.5 (Figure 3Bb), respectively. Thus, the structures of *syn*-HT-(+)- and (–)-**3**-Me (A) and *anti*-HH-(+)- and (–)-**4**-Me (B) were identified as shown in Figure 4A and B, respectively.

After the same photoreaction of **1**-Me on a large-scale, the four stereoisomers were successfully isolated by HPLC fractionation (see SI and Figure 3A). Among the four stereoisomers, two of them were further separated into two peaks due to the enantiomers by chiral HPLC (Figure 3B), which clearly revealed that these stereoisomers are unambiguously assigned to be either a *syn*-HT-**3**-Me or an *anti*-HH-**4**-Me photodimer. Both pairs of the enantiomers showed mirror image circular dichroism (CD) spectra and identical absorption spectra (Figure 3C). We then calculated the CD spectra of *syn*-HT and *anti*-HH photodimers of 2-phenylethynylanthracene as model photodimers of *syn*-HT-**3**-Me and *anti*-HH-**4**-Me, respectively, by the time-dependent density functional theory (TD-DFT) (Figure 4).[17] By comparison with the observed CD spectra, the structures of *syn*-HT-(+)- and (–)-**3**-Me and *anti*-HH-(+)- and (–)-**4**-Me were identified as shown in Figure 4A,B, respectively (see also Figure 3C). These results further indicated that the (+)-*syn*-HT-**3**-Me and (+)-*anti*-HH-**4**-Me dimers are most likely generated in a *si*-*si* HT and *re*-*re* HH fashion, respectively, during the intermolecular [4 + 4] photodimerization of **1**-Me.

In order to determine the structures of the other two isolated achiral photodimers (*anti*-HT-**2**-Me and *syn*-HH-**5**-Me), the $^1$H

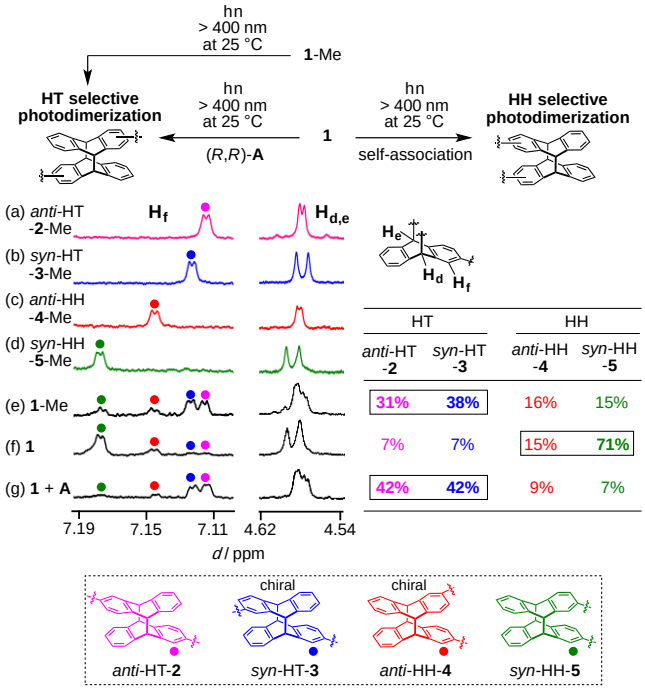


**Figure 5.** Partial $^1$H NMR spectra (500 MHz, $CDCl_3$, 25 °C) of isolated *anti*-HT-**2**-Me (a), *syn*-HT-**3**-Me (b), *anti*-HH-**4**-Me (c), *syn*-HH-**5**-Me (d), and (e–g) photodimers obtained after photoirradiation (> 400 nm) of **1**-Me (0.50 mM) (run 1, Table 1) (e) and **1** (0.50 mM) in the absence (run 2) (f) and presence of (*R*,*R*)-**A** (5.0 mM) (run 3) (g) in degassed $CDCl_3$ at 25 °C. The carboxylic acid photodimers obtained were isolated and converted to the methyl esters before NMR measurements (see SI). The peak assignments (e–g) were performed by comparing the $^1$H NMR spectra of the authentic photodimers (a–d).

NMR spectra of the isolated four photodimers were measured in benzene-$d_6$ (Figure S2B).[18] Among them, two of the four photodimers exhibited two nonequivalent doublet signals around 4.15 ppm with the characteristic coupling constant ($J$ = 11 Hz) for the bridge-head *anti*-vicinal protons ($H_d$ and $H_e$) as confirmed by measuring the $^1$H NMR spectra at different external magnetic field strengths, between which apparent cross-peaks were observed in the two-dimensional (2D) COSY spectra (Figure S2C,D). Hence, the structures of the two *anti*-stereoisomers (*anti*-HT-**2**-Me and *anti*-HH-**4**-Me) and then those of the two *syn*-stereoisomers (*syn*-HT-**3**-Me and *syn*-HH-**5**-Me) were unambiguously determined and their NMR spectra were clearly assigned as shown in Figures 5a-d and S2A.

Based on this structural information, it was revealed that **1**-Me photodimerized to afford sterically-favored HT dimers (*anti*-HT-**2**-Me and *syn*-HT-**3**-Me) as the major product (HT/HH = 69/31)[8a] after a 30-min photoirradiation in $CDCl_3$ at 25 °C, while the diastereoselectivity (*syn* and *anti*) was totally nonstereospecific as anticipated (run 1, Table 1).

**Template (T1)-Directed Photodimerization of 1.** We next examined the photodimerization of the carboxylic acid monomer (**1**) (0.50 mM) in degassed $CDCl_3$ at 25 °C in the absence and presence of the template joined by an achiral *p*-phenylene linker ((*R*,*R*,*R*,*R*)-**T1**) and monomeric amidine (*R*,*R*)-**A** (runs 2-4, Table 1). After irradiation of light (> 400 nm), the resulting carboxylic acid photodimers were isolated, then converted

**Table 1. Results of Photodimerizations of 1-Me and 1 (0.50 mM) in Degassed $CDCl_3$ at 25 °C**

| run | monomer | template (conc. (mM)) | irrad. time (min) | conv. (%) (consumption rate $10^{-3}$ $k$ ($s^{-1}$)) | relative yield (%)[a] (ee (%))[b] | | | | ratio[a] |
|---|---|---|---|---|---|---|---|---|---|
| | | | | | *anti*-HT-**2** | *syn*-HT-**3** | *anti*-HH-**4** | *syn*-HH-**5** | HT / HH |
| 1 | **1**-Me | - | 30 | 60 (0.46) | 31 | 38 | 16 | 15 | 69/31 |
| 2 | **1** | - | 10 | 60 (1.4) | 7 | 7 | 15 | 71 | 14/86 |
| 3 | | (*R*,*R*)-**A** (5.0) | 30 | 50 (0.40) | 42 | 42 (+6) | 9 (+5) | 7 | 84/16 |
| 4 | | (*R*,*R*,*R*,*R*)-**T1** (0.25) | 10 | 88 (3.4) | - | 73 (–48) | 22 (–16) | 5 | 73/27 |
| 5 | | (*R*,*R*,*S*,*S*,*R*,*R*)-**T2** (0.25) | 10 | 70 (2.1) | - | 87 (–40) | 13 (+8) | - | 87/13 |
| 6 | | (*S*,*S*,*S*,*S*,*S*,*S*)-**T3** (0.25) | 10 | 64 (1.7) | - | 85 (+28) | 15 (–6) | - | 85/15 |
| 7 | | (*R*,*R*,*R*,*R*,*R*,*R*)-**T4** (0.25) | 10 | 76 (2.8) | 25 | 25 (+14) | 43 (–62) | 7 | 50/50 |
| 8 | | (*R*,*R*,*S*,*S*,*R*,*R*)-**T5** (0.25) | 10 | 86 (3.3) | 23 | 23 (+26) | 40 (+24) | 14 | 46/54 |

[a]Estimated by $^1$H NMR as its methyl esters. [b]Determined by chiral HPLC (see Figure 3B). + and – denote the signs of the Cotton effect at 340 nm.

into the corresponding methyl esters by treatment with (trimethylsilyl)diazomethane, and the relative yields of the four stereoisomers were estimated by $^1$H NMR spectroscopy based on the $^1$H NMR spectra of the authentic photodimers (see SI and Figure 5a–d).

Interestingly, the photodimerization of **1** proceeded faster than that of **1**-Me to selectively yield the HH dimers (*anti*-HH-**4** and *syn*-HH-**5**) (HT/HH = 14/86), in particular, the *syn*-HH-**5** dimer in 71% yield after a 10-min irradiation (run 2, Table 1, Figures 5f and S3) probably due to the duplex formation ((**1**)$_2$) in a *syn*-HH fashion through self-association of the carboxy groups of **1** in $CDCl_3$ (Figure S4).[19,20]

The photodimerization of **1** (0.50 mM) in the presence of the *p*-phenylene-linked optically-active amidine template (*R*,*R*,*R*,*R*)-**T1** (0.25 mM) and its monomeric amidine (*R*,*R*)-**A** (0.50 mM) were then investigated in degassed $CDCl_3$ at 25 °C. The amidine monomer (*R*,*R*)-**A** was employed for the control experiment to evaluate the template effect of (*R*,*R*,*R*,*R*)-**T1** on the photodimerization. The $^1$H NMR spectra of **1** (0.50 mM) in the presence of (*R*,*R*)-**A** (0.50 mM) or (*R*,*R*,*R*,*R*)-**T1** (0.25 mM) exhibited the characteristic signals due to the NH protons in the low magnetic field at ca. 13.3 ppm, which clearly supported the salt bridge formations through which a 1:1 ((*R*,*R*)-**A**·**1**) or 1:2 ((*R*,*R*,*R*,*R*)-**T1**·(**1**)$_2$) complex was generated (Figures S7A and S9A). The CD spectra of the (*R*,*R*)-**A**·**1** and (*R*,*R*,*R*,*R*)-**T1**·(**1**)$_2$ complexes in $CDCl_3$ at 25 °C (Figure S5A,B) exhibited more intense Cotton effects than those of (*R*,*R*)-**A** and (*R*,*R*,*R*,*R*)-**T1** accompanied by an intense split-type Cotton effect that appeared in the absorption regions of the *m*-terphenyl units (ca. 230−300 nm), suggesting the duplex formation with a helix-sense bias, probably with an excess right-handed helical conformation induced by the chiral amidine residues with an (*R*)-configuration.[13a] In addition, the facts that the apparent Cotton effects were also induced in the absorption region of the achiral anthracene unit of **1** (450−350 nm) indicated that one or two anthracene units of **1** may be arranged in a chiral situation or a preferred-handed helical array upon complexation with (*R*,*R*)-**A** or along the (*R*,*R*,*R*,*R*)-**T1** template, respectively (Figure S5A,B). These Cotton effect signals almost remained unchanged even at 50 °C (Figure S6A,B).

The monomeric amidine (*R*,*R*)-**A** (5.0 mM) assisted the formation of the HT-photodimers (HT/HH = 84/16) with a negligible diastereoselectivity (*anti*/*syn* = ca. 1) (Figures 5g and S7Be) as observed in the photodimerization of **1**-Me together with low enantioselectivities (6 and 5% ee for *syn*-HT-**3** and *anti*-HH-**4**, respectively) (run 3, Table 1 and Figure S8).[21] In sharp contrast, the photodimerization of **1** in the presence of (*R*,*R*,*R*,*R*)-**T1** took place with high regio- (HT/HH = 73/27) and excellent diastereoselectivities (*anti*/*syn* = 0/73 (HT) and 22/5 (HH)) as well as an appreciable level of enantioselectivity, thus affording the chiral dimers of *syn*-HT-**3** and *anti*-HH-**4** in 73 and 22% relative yields with –48% and –16% ee, respectively (run 4, Table 1 and Figures 6a and S9).[22]

The observed high regio- and diastereoselective photodimerization of **1** in the presence of (*R*,*R*,*R*,*R*)-**T1**, predominantly giving the *syn*-HT-**3** dimer, could be ascribed to a reversible conformational change in the amidine dimer template between the zigzag- and crescent-shaped conformations that are in equilibrium (Figure 7); at high temperatures (> –30 °C), the equilibrium may be favorably shifted to the zigzag-shaped conformation (Figure 7A), in which two **1** monomers bind via

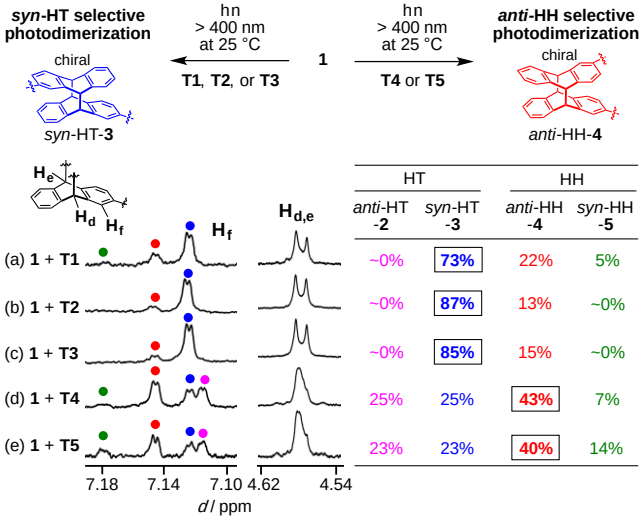


**Figure 6.** Partial $^1$H NMR spectra (500 MHz, $CDCl_3$, 25 °C) of photodimers obtained after irradiation of light (> 400 nm) of **1** (0.50 mM) in the presence of (*R*,*R*,*R*,*R*)-**T1** (0.25 mM) (run 4, Table 1) (a), (*R*,*R*,*S*,*S*,*R*,*R*)-**T2** (0.25 mM) (run 5) (b), (*S*,*S*,*S*,*S*,*S*,*S*)-**T3** (0.25 mM) (run 6) (c), (*R*,*R*,*R*,*R*,*R*,*R*)-**T4** (0.25 mM) (run 7) (d), and (*R*,*R*,*S*,*S*,*R*,*R*)-**T5** (0.25 mM) (run 8) (e) in degassed $CDCl_3$ at 25 °C. The carboxylic acid photodimers obtained were isolated and converted to the methyl esters before NMR measurements (see SI). The peak assignments (a–e) were performed by comparing the $^1$H NMR spectra of the authentic photodimers (Figure 5a–d).

salt bridges in such a way that the two anthracene units of **1** are preorganized to predominantly form a *re*-*re*-π-stacked dimer along the template, resulting in the *syn*-HT-**3** dimer rich in the (–)-enantiomer upon photoirradiation (Figures 7A and S10A). This speculation is supported by the calculated CD spectrum of a model dimer *syn*-HT' (Figure 4C) (for more details on the temperature-dependent photodimerization, see below and Table 2).

The photoreaction rate (*k*) of **1** in the presence of (*R*,*R*)-**A** was comparable to that of **1**-Me, but it was remarkably enhanced 7.4- and 8.5-folds in the presence of (*R*,*R*,*R*,*R*)-**T1** compared to those of **1**-Me and **1** in the absence of the template, respectively (runs 1-4, Table 1 and Figures S1C, S3D, S7D, and S9D).

**Effects of Linker Structures and Chirality on Template-Directed Photodimerization.** The effects of the linker structures and chiralities of a series of optically-active amidine dimer templates (**T2**–**T5** in Chart 1) on the template-directed photodimerization of **1** were then investigated under conditions identical to those shown in Figure 5 in terms of the reactivity of **1** and regio-, diastereo-, and enantioselectivities during the photodimerizations; the results are summarized in Table 1 (runs 5-8).

The introduction of the 2,5-di-(*S*)-2-methylbutoxy substituents at the *p*-phenylene linker of the **T1** template ((*R*,*R*,*S*,*S*,*R*,*R*)-**T2**) further enhanced the regio- (HT/HH = 87/13) and diastereoselectivities (*anti*/*syn* = 0/87 (HT) and 13/0 (HH)), yielding only the chiral *syn*-HT-**3** and *anti*-HH-**4** dimers in 87 and 13% relative yields with –40% and +8% ee, respectively (run 5, Table 1 and Figures 6b and S11). The enantioselectivity of the minor *anti*-HH-**4** dimer was inverted, which can be attributed to the linker chirality since both of the templates **T1** and **T2** are composed of the same (*R*,*R*)-amidine units.

To gain further insight, template (*S*,*S*,*S*,*S*,*S*,*S*)-**T3**, in which the (*R*,*R*)-amidine residues of (*R*,*R*,*S*,*S*,*R*,*R*)-**T2** were replaced by the opposite (*S*,*S*)-amidines, also assisted the *syn*-HT-**3**-selective chiral photodimer formation of **1** (*syn*-HT-**3** / *anti*-HH-**4** = 85/15). However, the enantioselectivities were completely reversed compared to those with (*R*,*R*,*S*,*S*,*R*,*R*)-**T2**, although the ee values of the chiral dimers (+28% and –6% ee for *syn*-HT-**3** and *anti*-HH-**4**, respectively) were lower than those with **T1** and **T2** (run 6, Table 1 and Figures 6c and S12). These results indicated that the amidine chirality of the templates **T1**–**T3** mainly contributed to the overall enantioselectivity during the photodimerization of **1**, while the linker chirality also plays a role, but may not be dominant over the amidine chirality. This speculation was supported by the fact that the CD spectrum of **T3** complexed with **1** was almost a mirror image to those of the **T1** and **T2** complexed with **1** both in the conjugated *m*-terphenyl and in the achiral anthracene chromophoric regions (Figure S5B-D), thereby switching the chirality of the *syn*-HT-**3** photodimer during the asymmetric photodimerization.

The photodimerization of **1** in the presence of templates consisting of the (*R*,*R*)-amidine dimers linked by the (*R*,*R*)- and (*S*,*S*)-*trans*-1,2-cyclohexanediamine through amide bonds ((*R*,*R*,*R*,*R*,*R*,*R*)-**T4** and (*R*,*R*,*S*,*S*,*R*,*R*)-**T5**, respectively) were then investigated. **T4** and **T5** (Figures S13 and S14) were previously used as versatile templates for the diastereoselective imine-bond forming reaction[13g] and duplex formation[13j] with racemic diamines and carboxylic acid dimers, respectively, through the complementary salt bridge formations. The DFT calculation combined with 2D NMR studies revealed that template **T5** formed a largely bent-shaped (kinked), right-handed double helix-like structure upon complexation with its complementary carboxylic acid dimer joined by the identical (*S*,*S*)-*trans*-1,2-cyclohexanediamine-based bis-amide linker (Figure S15),[13j] the structure of which is significantly different from those of the previously reported complementary double helices formed between chiral amidine dimers, such as **T1**, and achiral carboxylic acid dimers joined by phenylene or diacetylene linkages.[13h]

Therefore, we anticipated that the **T4** and **T5** templates likely formed 1:2 bent-shaped (kinked) duplexes with **1** through salt bridges, whose structures might be quite different from those of the other **T1**–**T3** templates complexed with **1** (Figure 7), in which the two anthracene units of **1** could be arranged along the templates in such a way to form both the HT- and HH-oriented π-stacked dimers. The relative orientation of two amidine residues of the templates seems to be responsible for this HT- or HH-regioselectivity as shown in Figure S16. In fact, the photoirradiation of **1** in the presence of **T4** and **T5** at 25 °C afforded all four dimers (HT/HH = 50/50 and 46/54, respectively) and the chiral *anti*-HH-**4** dimer was produced as the main product in 43 and 40% relative yields with –62% and +24% ee, respectively; the enantioselectivity was opposite to each other (runs 7 and 8, Table 1 and Figures 6d,e, S13, and S14). Based on the calculated CD spectrum of the model photodimer (Figure 4B), it can be assumed that the two prochiral anthracene units of **1** complexed with **T4** may be preorganized to form a *si*-*si* π-stacked dimer at 25 °C, thus generating the (–)-*anti*-HH-**4** enantiomer with a relatively high enantioselectivity (Figure S17A).

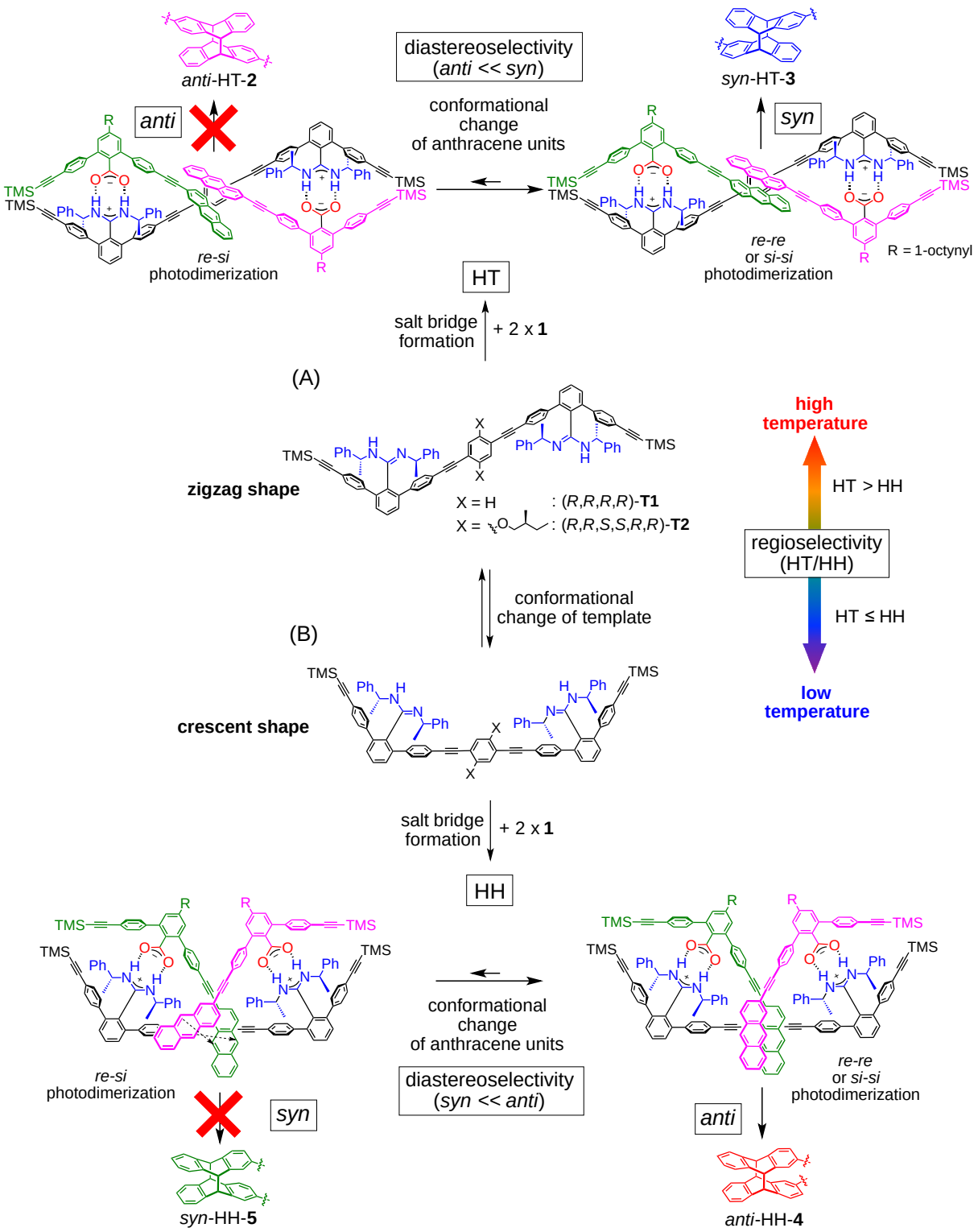


**Figure 7.** Possible mechanism for the regio- (HT or HH) and diastereo (*syn* or *anti*) selective photodimerization of **1** in the presence of (*R*,*R*,*R*,*R*)-**T1** and (*R*,*R*,*S*,*S*,*R*,*R*)-**T2** regulated by a reversible conformational change of the amidine dimer templates and anthracene units, resulting in the preferential formations of optically-active *syn*-HT-**3** (A) and *anti*-HH-**4** dimers (B).

The observed reversal in enantioselectivity between **T4** (–62% ee) and **T5** (+24% ee) indicated the dominant role of the chirality of the amide linkages ((*R*,*R*) and (*S*,*S*), respectively) in the formation of the chiral *anti*-HH-**4** dimer because both of the templates are composed of the same (*R*,*R*)-amidine dimer. However, the **T4** and **T5** templates promoted the formation of the chiral *syn*-HT-**3** dimer enriched in the same (+)-enantiomer with +14% and +26% ee, respectively (runs 7 and 8, Table 1 and Figure S17B), the chirality of which was opposite to that of the (–)-*syn*-HT-**3** dimer (–48% ee) produced in the presence of the phenylene-linked (*R*,*R*,*R*,*R*)-**T1** template composed of the (*R*,*R*)-amidine units (run 4, Table 1). These results suggest that both the amidine and amide linker chiralities of **T4** and **T5** contribute to the enantioselective photodimerization of **1**,

and such unique kinked structures of **T4** and **T5** (Figure S16), different from those of the other phenylene-linked amidine templates **T1**–**T3** (Figure 7) and showing reversible conformational changes in a different manner, may be responsible for the observed difference in the regio- and enantioselectivities. In other words, the suitable combination of chiral linkers and amidines will provide more efficient templates for achieving higher regio- and enantioselectivities during the template-directed photodimerization of **1**.

**Temperature Effects on Template-Directed Photodimerization.** The photodimerizations of **1** in the presence of the amidine templates (**T1**, **T2**, and **T4**) were then carried out in the temperature range between –50 and 50 °C to investigate the temperature effects on the regio-, diastereo-, and enantioselectivities during the template-directed photodimerization of **1**. These templates were selected because of their relatively high regio-, diastereo- and/or enantioselectivities at 25 °C (Table 1) and the results are summarized in Table 2.

The achiral (**T1**) and chiral (**T2**) *p*-phenylene-linked amidine dimers almost and exclusively afforded the chiral dimers of *syn*-HT-**3** and *anti*-HH-**4** as the major and minor products with moderate and low enantioselectivities, respectively, at 25 °C (runs 4 and 5, Table 1), regulated by a reversible conformational change in the amidine dimer templates between the zigzag- and crescent-shaped conformations as already mentioned (Figure 7). As anticipated, the equilibrium could be shifted to the zigzag-shaped conformation at high temperatures (Figure 7A), resulting in a more selective formation of the *syn*-HT-**3** dimer at 50 °C in 78 and 93% relative yields with similar enantioselectivities of –50% and –38% ee in the presence of **T1** and **T2**, respectively, while the formation of the *anti*-HH-**4** dimer remarkably increased with the decreasing temperature; the relative yields of the *anti*-HH-**4** dimer increased from 16 and 7% at 50 °C to 54 and 55% at –50 °C, respectively (runs 1-12, Table 2 and Figures S18A and 8A), probably due to the zigzag-to-crescent-shaped conformational change in the templates (Figure 7).

The **T1** and **T2** templates tended to produce the *syn*-HT-**3** photodimer with slight changes in the product ee (–50 to –30% and –38 to –24%, respectively) in the temperature range of 50 to –50 or –30 °C (Figures S18B and 8B) except for the *syn*-HT-**3** produced at –50 °C with **T2** showing the opposite chirality of the product (38% ee) (run 12, Table 2). This sudden and incoherent temperature-dependent chirality inversion of the *syn*-HT-**3** dimer may be due to the supramolecular aggregate formation of the ternary zigzag-shaped-**T2**·(**1**)$_2$ complex before photoirradiation (Figure S20). This assumption was supported by the fact that the photoirradiation of a dilute solution of **1** ([**T2**·(**1**)$_2$] = 0.025 mM) in the presence of **T2** at –50 °C afforded the *syn*-HT-**3** dimer with –30% ee (run 13, Table 2) comparable to those produced at –30 and –15 °C.

In contrast, the enantioselectivities of the *anti*-HH-**4** dimer assisted by **T1** and **T2** were highly dependent on the temperature and the ee of the *anti*-HH-**4** dimer in the presence of **T1** remarkably increased with the decreasing temperature, namely from –4% ee at 50 °C to a high ee value of –72% at –50 °C (runs 1-6, Table 2 and Figure S18C). A more significant temperature-dependent enhancement of the enantioselectivity of the *anti*-HH-**4** dimer accompanied by inversion of the product chirality was achieved upon photoirradiation of **1** in the presence of **T2**; the ee value of the *anti*-HH-**4** dimer produced at

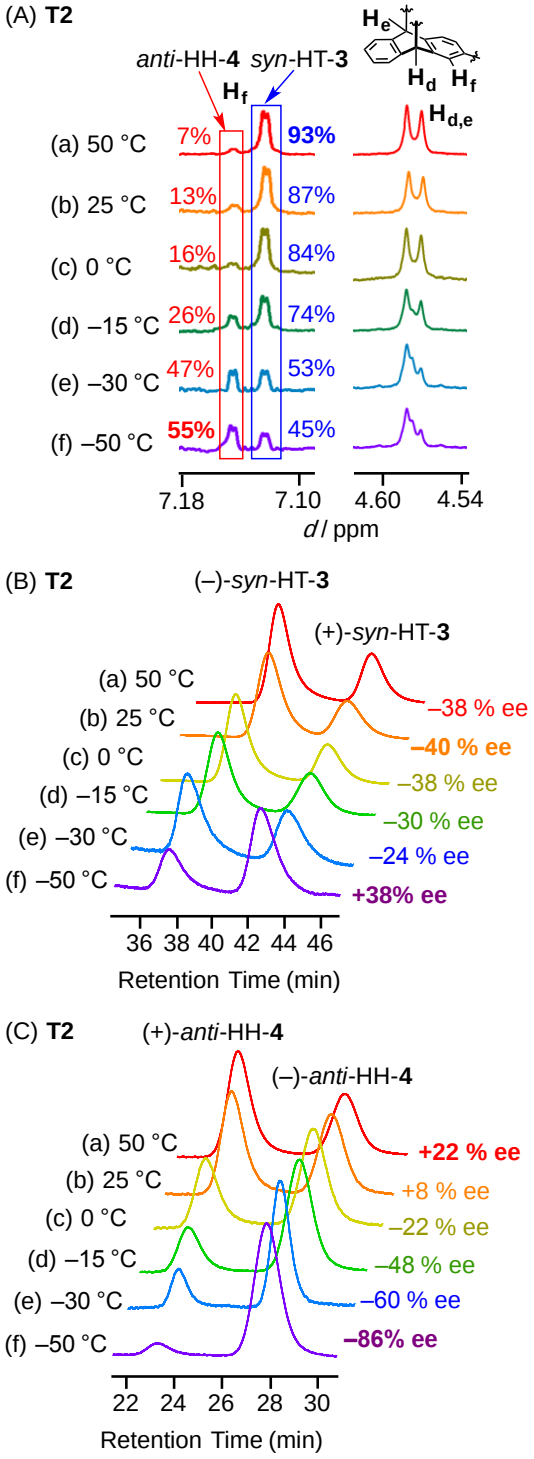


**Figure 8.** (A) Partial $^1$H NMR spectra (500 MHz, $CDCl_3$, 25 °C) of photodimers (*syn*-HT-**3** and *anti*-HH-**4**) (a–f) obtained after irradiation of light (> 400 nm) of **1** (0.50 mM) in the presence of (*R*,*R*,*S*,*S*,*R*,*R*)-**T2** (0.25 mM) in degassed $CDCl_3$ at 50 (a), 25 (b), 0 (c), –15 (d), –30 (e), and –50 °C (f) (runs 7-12, Table 2). The *syn*-HT-**3** and *anti*-HH-**4** photodimers obtained were isolated and converted to the methyl esters before NMR measurements (see SI). The peak assignments (a–f) were performed by comparing the $^1$H NMR spectra of the authentic photodimers (Figure 5a–d). (B,C) UV detected (270 nm) HPLC chromatograms for the resolution of the corresponding methyl esters of the isolated *syn*-HT-**3** (B) and *anti*-HH-**4** (C) (see Figure 3B). + and – denote the signs of the Cotton effect at 340 nm.

**Table 2. Results of Photodimerizations of 1 (0.50 mM) in the Presence of Chiral Templates in Degassed $CDCl_3$ at Various Temperatures**

| run | template (conc. (mM)) | temperature (°C) | irrad. time (min) | conv. (%) (consumption rate $10^{-3}$ $k$ ($s^{-1}$)) | relative yield (%)[a] (ee (%))[b] | | | | ratio[a] |
|---|---|---|---|---|---|---|---|---|---|
| | | | | | *anti*-HT-**2** | *syn*-HT-**3** | *anti*-HH-**4** | *syn*-HH-**5** | HT / HH |
| 1 | (*R*,*R*,*R*,*R*)-**T1** (0.25) | 50 | 10 | 92 (4.5) | - | 78 (–50) | 16 (–4) | 6 | 78/22 |
| 2 | | 25 | 10 | 88 (3.4) | - | 73 (–48) | 22 (–16) | 5 | 73/27 |
| 3 | | 0 | 10 | 82 (2.7) | - | 71 (–48) | 29 (–32) | - | 71/29 |
| 4 | | –15 | 10 | 72 (2.4) | - | 68 (–50) | 32 (–40) | - | 68/32 |
| 5 | | –30 | 15 | 60 (1.1) | - | 62 (–44) | 38 (–54) | - | 62/38 |
| 6 | | –50 | 15 | 50 (0.75) | - | 46 (–30) | 54 (–72) | - | 46/54 |
| 7 | (*R*,*R*,*S*,*S*,*R*,*R*)-**T2** (0.25) | 50 | 10 | 82 (2.7) | - | 93 (–38) | 7 (+22) | - | 93/7 |
| 8 | | 25 | 10 | 70 (2.1) | - | 87 (–40) | 13 (+8) | - | 87/13 |
| 9 | | 0 | 10 | 63 (1.6) | - | 84 (–38) | 16 (–22) | - | 84/16 |
| 10 | | –15 | 10 | 55 (1.1) | - | 74 (–30) | 26 (–48) | - | 74/26 |
| 11 | | –30 | 15 | 54 (0.90) | | 53 (–24) | 47 (–60) | | 53/47 |
| 12 | | –50 | 30 | 49 (0.49) | | 45 (+38) | 55 (–86) | | 45/55 |
| 13 | | –50[c] | 30 | 60 (-)[d] | | 45 (–30) | 55 (–86) | | 45/55 |
| 14 | (*R*,*R*,*R*,*R*,*R*,*R*)-**T4** (0.25) | 50 | 8 | 80 (3.3) | 27 | 21 (+8) | 40 (–54) | 12 | 48/52 |
| 15 | | 25 | 10 | 76 (2.8) | 25 | 25 (+14) | 43 (–62) | 7 | 50/50 |
| 16 | | 0 | 10 | 73 (2.4) | 27 | 22 (+14) | 46 (–70) | 5 | 49/51 |
| 17 | | –15 | 10 | 65 (1.7) | 23 | 20 (+20) | 49 (–78) | 8 | 43/57 |
| 18 | | –30 | 15 | 55 (0.90) | 22 | 20 (+20) | 54 (–84) | 4 | 42/58 |
| 19 | | –50 | 30 | 49 (0.46) | 17 | 17 (+22) | 60 (–88) | 6 | 34/66 |

[a]Estimated by $^1$H NMR as its methyl esters. [b]Determined by chiral HPLC (see Figure 3B). + and – denote the signs of the Cotton effect at 340 nm. [c][**1**] = 0.050 mM, [(*R*,*R*,*S*,*S*,*R*,*R*)-**T2**] = 0.025 mM. [d]It was difficult to estimate the comsumption rate by NMR because the concentration of **1** (0.050 mM) was too low.

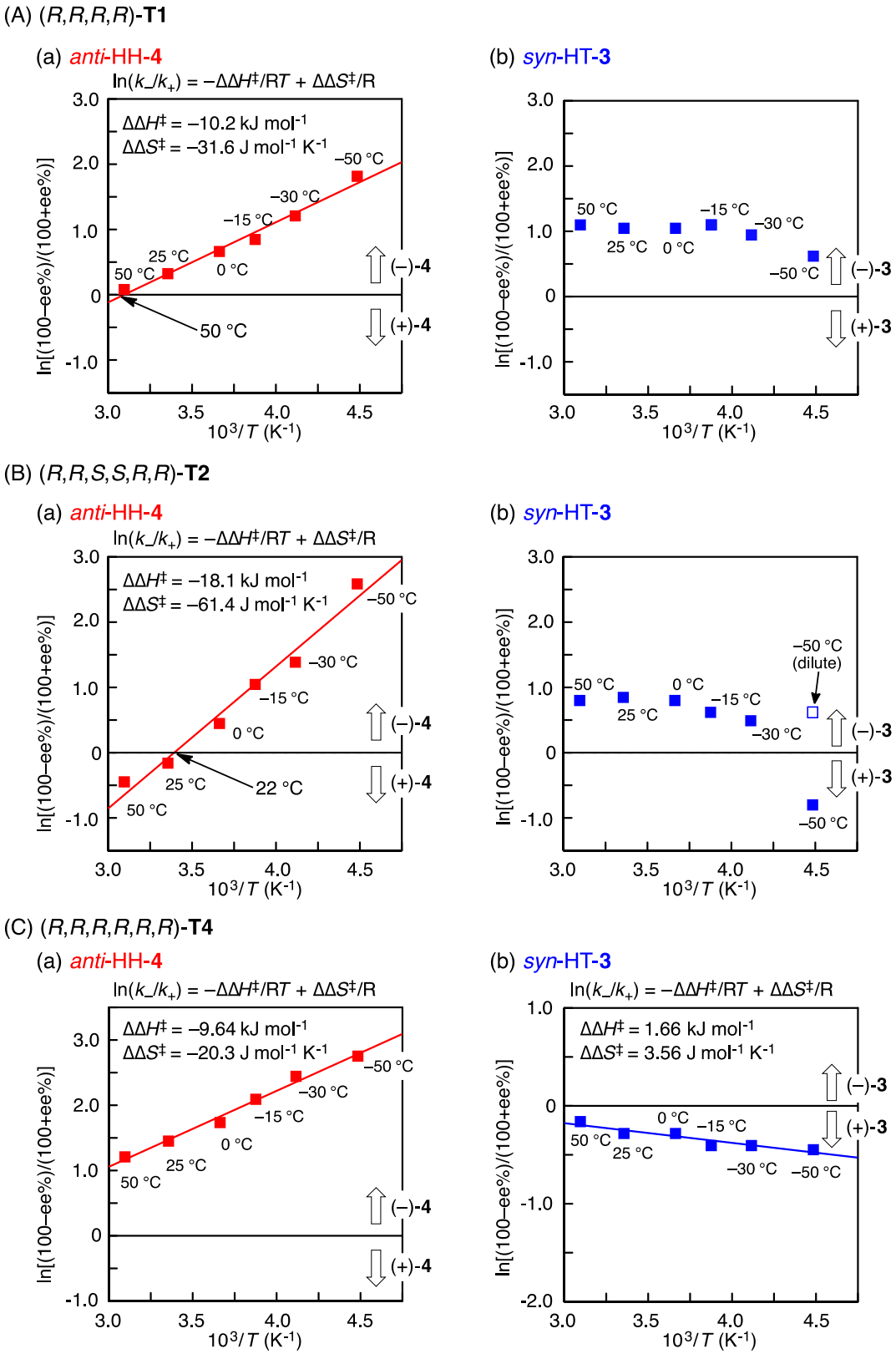


**Figure 9.** Plots of the natural logarithm of the relative yield of (+)- and (-)-enantiomers of *anti*-HH-**4** (a) and *syn*-HT-**3** (b) against the reciprocal temperature upon photoirradiation of **1** in the presence of (*R*,*R*,*R*,*R*)-**T1** (A), (*R*,*R*,*S*,*S*,*R*,*R*)-**T2** (B), and (*R*,*R*,*R*,*R*,*R*,*R*)-**T4** (C) (data are taken from Table 2). Differential activation parameters for the formations of enantiomeric *anti*-HH-**4** (a) (A-C) and *syn*-HT-**3** (Cb) estimated from the plots are also shown.

50 °C was +22%, which was inverted to the opposite –22% at 0 °C and eventually reached the higher value of –86% in the relative yield of 55% at –50 °C (Figure 8C).[23]

To gain insight into the origin of the temperature-dependence on the template-directed enantioselective photodimerizations of **1** in the presence of **T1** and **T2**, the natural logarithms of the relative enantiomer ratios of the (–)- and (+)-*syn*-HT-**3** and -*anti*-HH-**4** dimers, which represent the relative rate constants ($k_-/k_+$) for producing the (–)- and (+)-*syn*-HT-**3** and -*anti*-HH-**4** dimers, respectively, where $k_-/k_+$ = (100 – %ee)/(100 + %ee),[8c,j,24] were plotted versus the reciprocal temperature (1/*T*) to obtain the thermodynamic parameters ($\Delta\Delta H^{\ddagger}$ and $\Delta\Delta S^{\ddagger}$) from the linear plots based on the differential Eyring equation: $\ln(k_-/k_+) = -\Delta\Delta G^{\ddagger}/RT = -\Delta\Delta H^{\ddagger}/RT + \Delta\Delta S^{\ddagger}/R$, where the terms $\Delta\Delta G^{\ddagger}$, $\Delta\Delta H^{\ddagger}$, and $\Delta\Delta S^{\ddagger}$ represent the differential activation free energy, enthalpy, and entropy, respectively (Figure 9A,B).

As shown Figures 9Aa and Ba, the plots of $\ln(k_-/k_+)$ versus 1/*T* gave straight lines for the *anti*-HH-**4**, indicating a single enantiodifferentiation mechanism by which the enantioselective photodimerization of **1** proceeded along the crescent-shaped templates **T1** and **T2** (Figures 7B and S10B). The thermodynamic parameters $\Delta\Delta H^{\ddagger}$ and $\Delta\Delta S^{\ddagger}$ were then calculated from the slope and intercept, respectively, to be –10.2 kJ mol$^{-1}$ and –31.6 J mol$^{-1}$ K$^{-1}$ with **T1** and –18.1 kJ mol$^{-1}$ and –61.4 J mol$^{-1}$ K$^{-1}$ with **T2**. The same negative $\Delta\Delta H^{\ddagger}$ and $\Delta\Delta S^{\ddagger}$ values indicated the presence of a critical temperature (equipodal temperature ($T_0$)), at which the dominant enantiomer of *anti*-HH-**4** is switched, therefore, the $T_0$ values were estimated to be 50 (**T1**) and 22 °C (**T2**) based on the Gibbs–Helmholtz equation ($\Delta\Delta G^{\ddagger} = \Delta\Delta H^{\ddagger} - T\Delta\Delta S^{\ddagger}$).[8c,j,24] In the present enantioselective photodimerization of **1** in the presence of the amidine dimer templates of **T1** and **T2** at temperatures below $T_0$, the enthalpy difference $\Delta\Delta H^{\ddagger}$ attributed to doubly hydrogen bonded, amidinium-carboxylate salt bridges and face-to-face π-stacking of the anthracene residues of **1** mostly overcomes the entropy loss due to the mobility restriction through the salt bridge formation during the binding process.

A similar temperature-mediated inversion of the enantioselectivity of the chiral photodimers of 2-anthracenecarboxylic acid (AC) has been reported,[8c,j] but successful examples still remain limited to using modified CyD derivatives as the template,[8c,j] and we are still not aware of any hydrogen bond-based template systems that achieve inversion of the enantioselectivity of the chiral photodimers of prochiral anthracenes during asymmetric photoreactions. On the other hand, the Eyring plots of the enantiomer ratios of the *syn*-HT-**3** dimer did not give a good straight line (Figure 9Ab,Bb). The reason is not clear at present, but may be ascribed to the aggregate formation of the ternary zigzag-shaped **T1**·(**1**)$_2$ and **T2**·(**1**)$_2$ complexes in solution at low temperatures (Figure S20).

A similar enhancement of the *anti*-HH-**4** dimer formation together with the enantioselectivity at low temperatures was also observed for the amide-linked template **T4**, producing the *anti*-HH-**4** dimer in 60% relative yield with the highest ee value of –88 % at –50 °C (runs 14-19 in Table 2 and Figure S19), which is, to the best of our knowledge, among the highest ee value reported for hydrogen bond-based template-assisted photodimerizations of 2-substituted anthracenes.[9] Plots of the logarithms of the enantiomer ratios of *syn*-HT-**3** and *anti*-HH-**4** versus 1/*T* gave good straight lines (Figure 9C), although an equipodal temperature ($T_0$) could not be observed in the temperature range between –50 and 50 °C.

## CONCLUSION

In conclusion, the present findings revealed that the complementary amidinium–carboxylate salt bridges indeed work as a versatile scaffold to provide a unique and rare example of the successful template-directed photodimerization of a prochiral anthracene in highly regio-, diastereo-, and enantioselective fashions. Further development of more efficient chiral templates for achieving higher regio-, diastereo-, and enantioselectivities during the template-directed photodimerization of **1** at an appropriate temperature will be possible by the suitable combination of chiral amidines and linkers. We believe that the present findings will also provide a possible strategy for realizing more sophisticated asymmetric photodimerizations of prochiral anthracenes[8g,h,10d] in the presence of a catalytic amount of chiral amidine dimers or chiral/achiral amidine dimers as a template, through which chiral amplification will be also operative in the latter case during complementary amidinium-carboxylate salt bridge formations.[9e,13c,f,25]

## ASSOCIATED CONTENT

### Supporting Information

The Supporting Information is available free of charge on the ACS Publications website.

Experimental procedures, characterizations of dimer strands, and additional spectroscopic data (PDF)

## AUTHOR INFORMATION


### Corresponding Author

*yashima@chembio.nagoya-u.ac.jp

### Present Address

†Department of Molecular and Macromolecular Chemistry, Graduate School of Engineering, Nagoya University, Chikusa-ku, Nagoya 464-8603, Japan.


### Notes

The authors declare no competing financial interest.

## ACKNOWLEDGMENT


This work was supported in part by JSPS KAKENHI (Grant-in-Aid for Scientific Research (S), no. 25220804 (E.Y.) and Grant-in-Aid for Young Scientists (B), no. 16K17892 (D.T.)). J.T. expresses his thanks for the JSPS Research Fellowship for Young Scientists (no. 8886).


## REFERENCES


(1) (a) Hoffmann, N. *Chem. Rev.* **2008**, *108*, 1052-1103. (b) Bach, T.; Hehn, J. P. *Angew. Chem., Int. Ed.* **2011**, *50*, 1000-1045. (c) Hoffmann, N. *J. Photochem. Photobiol., C: Photochem. Rev.* **2014**, *19*, 1-19. (d) Hoffmann, N. *Synthesis* **2016**, *48*, 1782-1802.

(2) Reviews on template-directed photochemical reactions: (a) McClenaghan, N. D.; Bassani, D. M. *Int. J. Photoenergy* **2004**, *6*, 185-192. (b) Svoboda, J.; König, B. *Chem. Rev.* **2006**, *106*, 5413-5430. (c) Yang, C. *Chin. Chem. Lett.* **2013**, *24*, 437-441. (d) Bibal, B.; Mongin, C.; Bassani, D. M. *Chem. Soc. Rev.* **2014**, *43*, 4179-4198. (e) Vallavoju, N.; Sivaguru, J. *Chem. Soc. Rev.* **2014**, *43*, 4084-4101. (f) Yang, C.; Inoue, Y. *Chem. Soc. Rev.* **2014**, *43*, 4123-4143. (g) Brimioulle, R.; Lenhart, D.; Maturi, M. M.; Bach, T. *Angew. Chem.*,

*Int. Ed.* **2015**, *54*, 3872-3890. (h) Ramamurthy, V.; Sivaguru, J. *Chem. Rev.* **2016**, *116*, 9914-9993.

(3) Reviews on photodimerization of anthracene derivatives: (a) Becker, H.-D. *Chem. Rev.*, **1993**, *93*, 145-172. (b) Bouas-Laurent, H.; Castellan, A.; Desvergne, J.-P.; Lapouyade, R. *Chem. Soc. Rev.* **2000**, *29*, 43-55. (c) Bouas-Laurent, H.; Castellan, A.; Desvergne, J.-P.; Lapouyade, R. *Chem. Soc. Rev.* **2001**, *30*, 248-263.

(4) (a) Tamaki, T. *Chem. Lett.* **1984**, 53-56. (b) Tamaki, T.; Kokubu, T. *J. Inclusion Phenom.* **1984**, *2*, 815-822. (c) Tamaki, T.; Kokubu, T.; Ichimura, K. *Tetrahedron* **1987**, *43*, 1485-1494.

(5) (a) Ueno, A.; Moriwaki, F.; Iwama, Y.; Suzuki, I.; Osa, T.; Ohta, T.; Nozoe, S. *J. Am. Chem. Soc.* **1991**, *113*, 7034-7036. (b) Ikeda, H.; Nihei, T.; Ueno, A. *J. Org. Chem.* **2005**, *70*, 1237-1242.

(6) (a) Dawn, A.; Fujita, N.; Haraguchi, S.; Sada, K.; Shinkai, S. *Chem. Commun.* **2009**, 2100-2102. (b) Dawn, A.; Shiraki, T.; Haraguchi, S.; Sato, H.; Sada, K.; Shinkai, S. *Chem. - Eur. J.* **2010**, *16*, 3676-3689.

(7) Alagesan, M.; Kanagaraj, K.; Wan, S.; Sun, H.; Su, D.; Zhong, Z.; Zhou, D.; Wu, W.; Gao, G.; Zhang, H.; Yang, C. *J. Photochem. Photobiol., A: Chem.* **2016**, *331*, 95-101.

(8) (a) Nakamura, A.; Inoue, Y. *J. Am. Chem. Soc.* **2003**, *125*, 966-972. (b) Nakamura, A.; Inoue, Y. *J. Am. Chem. Soc.* **2005**, *127*, 5338-5339. (c) Yang, C.; Fukuhara, G.; Nakamura, A.; Origane, Y.; Fujita, K.; Yuan, D.-Q.; Mori, T.; Wada, T.; Inoue, Y. *J. Photochem. Photobiol., A: Chem.* **2005**, *173*, 375-383. (d) Yang, C.; Nakamura, A.; Fukuhara, G.; Origane, Y.; Mori, T.; Wada, T.; Inoue, Y. *J. Org. Chem.* **2006**, *71*, 3126-3136. (e) Yang, C.; Mori, T.; Inoue, Y. *J. Org. Chem.* **2008**, *73*, 5786-5794. (f) Yang, C.; Mori, T.; Origane, Y.; Ko, Y. H.; Selvapalam, N.; Kim, K.; Inoue, Y. *J. Am. Chem. Soc.* **2008**, *130*, 8574-8575. (g) Ke, C. F.; Yang, C.; Mori, T.; Wada, T.; Liu, Y.; Inoue, Y. *Angew. Chem., Int. Ed.* **2009**, *48*, 6675-6677. (h) Wang, Q. A.; Yang, C.; Fukuhara, G.; Mori, T.; Liu, Y.; Inoue, Y. *Beilstein J. Org. Chem.* **2011**, *7*, 290-297. (i) Yang, C.; Ke, C. F.; Liang, W. T.; Fukuhara, G.; Mori, T.; Liu, Y.; Inoue, Y. *J. Am. Chem. Soc.* **2011**, *133*, 13786-13789. (j) Yao, J. B.; Yan, Z. Q.; Ji, J. C.; Wu, W. H.; Yang, C.; Nishijima, M.; Fukuhara, G.; Mori, T.; Inoue, Y. *J. Am. Chem. Soc.* **2014**, *136*, 6916-6919.

(9) (a) Mizoguchi, J.-i.; Kawanami, Y.; Wada, T.; Kodama, K.; Anzai, K.; Yanagi, T.; Inoue, Y. *Org. Lett.* **2006**, *8*, 6051-6054. (b) Kawanami, Y.; Pace, T. C. S.; Mizoguchi, J.-i.; Yanagi, T.; Nishijima, M.; Mori, T.; Wada, T.; Bohne, C.; Inoue, Y. *J. Org. Chem.* **2009**, *74*, 7908-7921. (c) Kawanami, Y.; Katsumata, S.-y.; Mizoguchi, J.-i.; Nishijima, M.; Fukuhara, G.; Yang, C.; Mori, T.; Inoue, Y. *Org. Lett.* **2012**, *14*, 4962-4965. (d) Kawanami, Y.; Umehara, H.; Mizoguchi, J.-i.; Nishijima, M.; Fukuhara, G.; Yang, C.; Mori, T.; Inoue, Y. *J. Org. Chem.* **2013**, *78*, 3073-3085. (e) Kawanami, Y.; Katsumata, S.-y.; Nishijima, M.; Fukuhara, G.; Asano, K.; Suzuki, T.; Yang, C.; Nakamura, A.; Mori, T.; Inoue, Y. *J. Am. Chem. Soc.* **2016**, *138*, 12187-12201.

(10) (a) Wada, T.; Nishijima, M.; Fujisawa, T.; Sugahara, N.; Mori, T.; Nakamura, A.; Inoue, Y. *J. Am. Chem. Soc.* **2003**, *125*, 7492-7493. (b) Nishijima, M.; Wada, T.; Mori, T.; Pace, T. C. S.; Bohne, C.; Inoue, Y. *J. Am. Chem. Soc.* **2007**, *129*, 3478-3479. (c) Fuentealba, D.; Kato, H.; Nishijima, M.; Fukuhara, G.; Mori, T.; Inoue, Y.; Bohne, C. *J. Am. Chem. Soc.* **2013**, *135*, 203-209. (d) Nishijima, M.; Kato, H.; Yang, C.; Fukuhara, G.; Mori, T.; Araki, Y.; Wada, T.; Inoue, Y. *ChemCatChem* **2013**, *5*, 3237-3240. (e) Nishijima, M.; Goto, M.; Fujikawa, M.; Yang, C.; Mori, T.; Wada, T.; Inoue, Y. *Chem. Commun.* **2014**, *50*, 14082-14085.

(11) (a) Ishida, Y.; Kai, Y.; Kato, S.-y.; Misawa, A.; Amano, S.; Matsuoka, Y.; Saigo, K. *Angew. Chem., Int. Ed.* **2008**, *47*, 8241-8245. (b) Ishida, Y.; Achalkumar, A. S.; Kato, S.-y.; Kai, Y.; Misawa, A.; Hayashi, Y.; Yamada, K.; Matsuoka, Y.; Shiro, M.; Saigo, K. *J. Am. Chem. Soc.* **2010**, *132*, 17435-17446. (c) Ishida, Y.; Matsuoka, Y.; Kai, Y.; Yamada, K.; Nakagawa, K.; Asahi, T.; Saigo, K. *J. Am. Chem. Soc.* **2013**, *135*, 6407-6410.

(12) (a) Fukuhara, G.; Nakamura, T.; Kawanami, Y.; Yang, C.; Mori, T.; Hiramatsu, H.; Dan-oh, Y.; Tsujimoto, K.; Inoue, Y. *Chem. Commun.* **2012**, *48*, 9156-9158. (b) Fukuhara, G.; Nakamura, T.; Kawanami, Y.; Yang, C.; Mori, T.; Hiramatsu, H.; Dan-oh, Y.; Nishimoto, T.; Tsujimoto, K.; Inoue, Y. *J. Org. Chem.* **2013**, *78*, 10996-11006. (c) Fukuhara, G.; Iida, K.; Kawanami, Y.; Tanaka, H.; Mori, T.; Inoue, Y. *J. Am. Chem. Soc.* **2015**, *137*, 15007-15014. (d) Fukuhara, G.; Iida, K.; Mori, T.; Inoue, Y. *J. Photochem. Photobiol., A.: Chem.* **2016**, *331*, 76-83.

(13) (a) Tanaka, Y.; Katagiri, H.; Furusho, Y.; Yashima, E. *Angew. Chem., Int. Ed.* **2005**, *44*, 3867-3870. (b) Hasegawa, T.; Furusho, Y.; Katagiri, H.; Yashima, E. *Angew. Chem., Int. Ed.* **2007**, *46*, 5885-5888. (c) Ito, H.; Furusho, Y.; Hasegawa, T.; Yashima, E. *J. Am. Chem. Soc.* **2008**, *130*, 14008-14015. (d) Maeda, T.; Furusho, Y.; Sakurai, S.-i.; Kumaki, J.; Okoshi, K.; Yashima, E. *J. Am. Chem. Soc.* **2008**, *130*, 7938-7945. (e) Yamada, H.; Furusho, Y.; Ito, H.; Yashima, E. *Chem. Commun.* **2010**, *46*, 3487-3489. (f) Ito, H.; Ikeda, M.; Hasegawa, T.; Furusho, Y.; Yashima, E. *J. Am. Chem. Soc.* **2011**, *133*, 3419-3432. (g) Yamada, H.; Furusho, Y.; Yashima, E. *J. Am. Chem. Soc.* **2012**, *134*, 7250-7253. (h) Yamada, H.; Wu, Z.-Q.; Furusho, Y.; Yashima, E. *J. Am. Chem. Soc.* **2012**, *134*, 9506-9520. (i) Tanabe, J.; Taura, D.; Yamada, H.; Furusho, Y.; Yashima, E. *Chem. Sci.* **2013**, *4*, 2960-2966. (j) Makiguchi, W.; Tanabe, J.; Yamada, H.; Iida, H.; Taura, D.; Ousaka, N.; Yashima, E. *Nat. Commun.* **2015**, *6*, 7236; DOI: 10.1038/ncomms8236. (k) Tanabe, J.; Taura, D.; Ousaka, N.; Yashima, E. *Org. Biomol. Chem.* **2016**, *14*, 10822-10832. (l) Taura, D.; Hioki, S.; Tanabe, J.; Ousaka, N.; Yashima, E. *ACS Catal.* **2016**, *6*, 4685-4689.

(14) We recently reported a remarkable template effect of **T1** on the photodimerization of two achiral carboxylic acid monomers bearing a 9-substituted anthracene residue at one and both ends, resulting in the formation of achiral [4 + 4]- and [4 + 2]-*anti* photodimers, which were preferentially produced with 30- and 61-times accelerations of the dimerization reactions, respectively, due to the complementary amidinium–carboxylate salt bridge formation.[13k]

(15) Another [4 + 2] photodimer formation due to a [4 + 2] Diels-Alder addition reaction[16] between the ethynyl residue of **1**-Me and the central ring of the other anthracene moiety may be possible, since such a [4 + 2] photodimer formation occurred during the photodimerization of an analogous monomer like **1**-Me in which the anthracene unit was attached at the 9-position.[13k] However, this possibility could be ruled out because no trace of such [4 + 2] photodimer was detected by $^1$H NMR spectroscopy.

(16) Becker, H.-D.; Andersson, K. *J. Photochem.* **1984**, *26*, 75-77.

(17) Wakai, A.; Fukasawa, H.; Yang, C.; Mori, T.; Inoue, Y. *J. Am. Chem. Soc.* **2012**, *134*, 4990-4997.

(18) Benzene-$d_6$ was used as a solvent because the chemical shifts of the bridge-head-vicinal protons ($H_d$ and $H_e$) in $CDCl_3$ were too close to identify if they were two singlet (*syn*) or doublet (*anti*) as shown in Figure S2A.

(19) (a) Makiguchi, W.; Kobayashi, S.; Furusho, Y.; Yashima, E. *Angew. Chem., Int. Ed.* **2013**, *52*, 5275-5279. (b) Makiguchi, W.; Kobayashi, S.; Furukawa, K.; Iida, H.; Furusho, Y.; Yashima, E. *J. Polym. Sci., Part A: Polym. Chem.* **2015**, *53*, 990-999.

(20) The energy-minimized structure of the self-associated (**1**)$_2$ optimized by the DFT calculation revealed that the two anthracene units of (**1**)$_2$ were favorably arranged in a *syn*-HH fashion as shown in Figure S4. The initial structure of (**1**)$_2$, in which the two anthracene units were constructed in such a way to form an *anti*-HH precursor, was also optimized by the DFT calculation, but the resulting energy-minimized structure after the calculation was identical to that of the *syn*-HH precursor (Figure S4).

(21) Photoirradiation of **1** in the presence of (*R*,*R*)-**A** (0.50 mM) in $CDCl_3$ at 25 °C for 30 min generated a very small amount of hydrochloric acid to form a hydrochloride salt of (*R*,*R*)-**A** (ca. 7 mol%), which gave rise to dissociation of the (*R*,*R*)-**A**·**1** complex. Therefore, we used an excess amount of (*R*,*R*)-**A** (5.0 mM) in the control experiment in order to avoid the effect of hydrochloric acid during the photodimerization reaction. We noted that no trace amount of hydrochloric acid was generated after the photoirradiation of **1** in $CDCl_3$ at 25 °C for 10 min and at low temperature below –30 °C for 30 min.

(22) The photodimerizations of **1** in the presence of (*R*,*R*,*R*,*R*)-**T1** in $CD_2Cl_2$ and toluene-$d_8$ at 25 °C produced the photodimers in a similar regio-, diastereo-, and enantioselective manner as in $CDCl_3$, affording the achiral *syn*-HH-**5** in 5 and 7% relative yields, and chiral

*syn*-HT-**3** and *anti*-HH-**4** in 84 (–50% ee) and 74 (–56% ee), and 11% (–14% ee) and 19% (–14% ee) relative yields, respectively.

(23) The variable-temperature absorption/CD and $^1$H NMR measurements of **T2** and its complex with **1** in $CDCl_3$ were performed in the temperature range between –60 and 25 °C in order to observe the equilibrium between the zigzag- and crescent-shaped conformations of **T2** (Figure 7). The absorption and CD spectral patterns and intensities of **T2** and its complex with **1** were more or less changed and their $^1$H NMR chemical shifts were also changed with broadening of the proton resonances upon cooling, but we could not observe clear isosbestic points and a coalescence temperature showing such conformational changes in **T2** based on the variable-temperature absorption/CD and $^1$H NMR spectral changes, respectively.

(24) Inoue, Y. *Chem. Rev.* **1992,** *92*, 741-770.

(25) (a) Yashima, E.; Maeda, K.; Iida, H.; Furusho, Y.; Nagai, K. *Chem. Rev.* **2009**, *109*, 6102-6211. (b) Yashima, E.; Ousaka, N.; Taura, D.; Shimomura, K.; Ikai, T.; Maeda, K. *Chem. Rev.* **2016**, *116*, 13752-13990.

**Table of Contents Artwork**

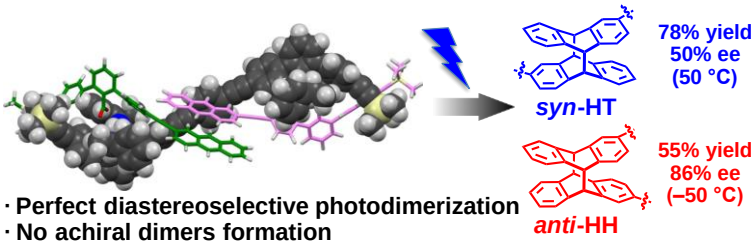


· Perfect diastereoselective photodimerization
· No achiral dimers formation